Multi-Stage Regulation, a Key to Reliable Adaptive Biochemical Pathways

Gal Almogy,*† Lewi Stone,* and Nir Ben-Tal†
*Biomathematics Unit, Department of Zoology and †Department of Biochemistry, The George S. Wise Faculty of Life Sciences, Tel Aviv University, Ramat Aviv 69978, Israel

ABSTRACT A general "multi-stage" regulation model, based on linearly connected regulatory units, is formulated to demonstrate how biochemical pathways may achieve high levels of accuracy. The general mechanism, which is robust to changes in biochemical parameters, such as protein concentration and kinetic rate constants, is incorporated into a mathematical model of the bacterial chemotaxis network and provides a new framework for explaining regulation and adaptiveness in this extensively studied system. Although conventional theories suggest that methylation feedback pathways are responsible for chemotactic regulation, the model, which is deduced from known experimental data, indicates that protein interactions downstream of the bacterial receptor complex, such as CheAs and CheZ, may play a crucial and complementary role.

INTRODUCTION

Given the rapidity with which signal transduction pathways and genetic circuits are being unraveled, it has become increasingly important to attain a theoretical understanding of the dynamics of these complex biological systems (Lamb, 1996; Lauffenburger, 2000; Edwards et al., 2001). A generic constraint on cellular machines is the inherent inexactness of the computational elements comprising a biological regulation unit (Bray, 1995). As such, accounting for the apparent precision of many biological processes has proven to be a major conceptual difficulty and has been the goal of numerous mathematical modeling studies (Segel et al., 1986; Bray et al., 1993; Bray and Bourret, 1995; Hauri and Ross, 1995; Barkai and Leibler, 1997; Spiro et al., 1997). In an attempt to resolve this problem, we explore the well-elucidated bacterial chemotaxis network in *Escherichia coli* from a modeling perspective that takes into account recent new findings concerning protein interactions and their potential regulatory roles.

The bacterium *E. coli* responds to changes in the concentration of various chemicals in its environment (Eisenbach, 1996; Stock and Surrete, 1996; Bren and Eisenbach, 2000; Robinson et al. 2000; Falke and Hazelbauer, 2001). An individual cell swims along a smooth trajectory, tumbles erratically for a brief time, choosing randomly a new direction, and then swims smoothly again. If a certain run happens to carry the cell up a gradient of a nutrient consumed by the cell, referred to as attractant, then the occupancy of the appropriate chemoreceptor is increased and a "swim" signal is generated. Likewise, a "tumble" signal (CheYp molecule) is generated for bacteria swimming up a gradient of a repellent. Note that our knowledge of these responses stems from laboratory studies where tests are usually made only under artificially imposed steep gradients of repellent concentration (Berg and Brown, 1972; Block et al., 1983), rather than the smaller gradients associated with natural environmental conditions. Bacterial motion is governed by a sophisticated motor (~6 per cell), which is attached to a long helical flagellum (Macnab, 2001; Samatey et al., 2001). When the motors turn the flagella counter-clockwise (CCW), there is a high probability that the flagella will form a bundle rotating in the same direction, causing the bacteria to shoot forward. In contrast, when the flagella turn clockwise (CW), they generally move separately, thereby causing the bacteria to tumble. In fact, Berg and co-workers have shown recently that even a single flagellum turning CCW can cause bacteria to swim smoothly (Turner et al., 2000). The direction of rotation the motor will assume is determined by the CheYp–motor interaction, which has a large Hill coefficient (~10, Cluzel et al., 2000) and hence is highly sensitive to CheYp concentration. Although this may facilitate a rapid and sizable response of the bacteria to minute changes in the external environment, it necessitates precise regulation of the CheYp level to keep the bacteria from being constantly locked in either the swimming or tumbling state. This is especially true given the remarkable ability of the bacterial chemotaxis system to adapt precisely to high concentrations of various substances in close physical proximity (Stock and Surrete, 1996; Alon et al., 1999). This ability, however, is not constant to all stimuli, and some stimuli produce a more exact response than others. That is, while abrupt long-term (or even permanent) changes in environment cause temporary shifts in the bacteria's swim-to-tumble ratio, the final steady-state behavior of the bacteria in many cases remains unchanged—a phenomenon that is termed exact adaptation.

Under normal physiological conditions, bacteria are mostly subjected to minor gradient changes. Under these

Received for publication 30 August 2000 and in final form 23 July 2001.
Address reprint requests to Nir Ben-Tal, Dept. of Biochemistry, The George S. Wise Faculty of Life Sciences, Tel Aviv University, Ramat Aviv 69978, Israel. Tel.: +972-3-640-6709; Fax: +972-3-640-6834; E-mail: bental@ashtoret.tau.ac.il; web: http://ashtoret.tau.ac.il/.

0006-3495/01/12/3016/13 $2.00

conditions, the chemotactic mechanism is able to rapidly terminate the response (e.g., elevated CheYp level) on the time-scale of seconds (Segall et al., 1986; Stock and Surrete, n1996). This rapid adaptation is the major quality required for typical physiological changes. In contrast, bacteria are also able to adapt to drastic changes of over 5 orders of magnitude in their chemical environment (Stock and Surrete, 1996). Adapting to these rare, large-scale changes requires a robust, highly exact mechanism (Stock and Surrete, 1996), because it has to restore CheYp initial level in the face of a significantly altered chemical environment. Note that the rapidity of adaptation emphasized earlier is immaterial in these rare cases.

Until now, the adaptation mechanisms in models of bacterial chemotaxis have been based on methylation-dependent processes (Asakura and Honda, 1984; Bray et al., 1993; Hauri and Ross, 1995; Barkai and Leibler, 1997; Spiro et al., 1997). In nearly all studies (but see Asakura and Honda, 1984), models were "fine-tuned" (Bray et al., 1993; Hauri and Ross, 1995; Spiro et al., 1997) and could only demonstrate exact adaptation in narrow regions of parameter space. Barkai and Leibler (1997) and Yi et al. (2000) have recently demonstrated that biochemical networks, tightly controlled through feedback of methylation/demethylation pathways, can achieve exact adaptation that is robust to parameter variation. Since then, experimental findings have strongly supported the "robust" approach to modeling bacterial chemotaxis (Alon et al., 1999). However, there is now growing experimental evidence that, in a number of important circumstances, the adaptive behavior of bacteria does not strongly depend on methylation–demethylation feedback processes and has therefore been termed "methylation independent" (Stock et al., 1985; Armitage, 1993). We present such an alternative methylation-independent mechanism that accounts for both exactness and rapidity of adaptation—the two qualities required for efficient chemotactic behavior (Alon et al., 1999; Segall et al., 1982).

METHYLATION-INDEPENDENT ADAPTATION

The actual quantity regulated in the chemotactic process is the ratio of swim-to-tumble periods, directly determined by the CheYp concentration (Stock and Surrete, 1996). Previous models of chemotactic adaptation, based on the methylation/demethylation feedback, only model the regulation of the receptor activity. In contrast, the model presented here is based on recent knowledge of the complex dynamics of CheYp, both phosphorylation and dephosphorylation, which also affect chemotactic adaptation.

The literature indicates that the dynamics of CheYp is more complex than previously modeled. Recent evidence suggests that there are, in fact, two separate pathways for CheYp dephosphorylation (Fig. 1). It is now understood that CheYp enhances the protein CheZ's dephosphorylating activity by an as yet unidentified mechanism (Blat et al., 1998). Conversely, CheZ is well known to rapidly dephosphorylate CheYp, thereby diminishing CheYp concentration (Eisenbach, 1996). Furthermore, it has been demonstrated that CheAs (short form of CheA, an essential part of the receptor complex) interacts with CheZ to form a stable CheAs–CheZ complex (Wang and Matsumura, 1997) that is an order of magnitude more active in dephosphorylating CheYp than CheZ alone (Wang and Matsumura, 1996). CheAs over-expression in vivo causes a strong CCW bias, as expected in the presence of excessive dephosphorylation (Wang and Matsumura, 1996). Under optimal motility conditions, the CheAs/CheA ratio is 1:1 (Bren and Eisenbach, 2000). Finally, CheZ and CheAs have a regular expression correlation (McNamara and Wolfe, 1996); that is, a bacteria either has both CheZ and CheAs or neither, implying a functional relationship between the two proteins. Note that, in Bacteria where CheZ is absent, there is usually a variant form of either CheZ or CheY that serves in the CheYp dephosphorylation (Stock and Surrete, 1996).

In an attempt to account for reports of methylation-independent regulation, the model proposed here examines the possibility that there are two linearly connected regulation stages as depicted in Fig. 1 *A*. The conventional "primary stage" regulates the methylation level of the receptor complex by the CheR and CheB proteins, thus controlling the receptor activity and the phosphorylation rate of CheY. The secondary regulatory stage controls the dephosphorylation rate of CheYp, and thus may also have significant influence on chemotactic adaptation. It consists of two parallel feedback loops, as indicated in Fig. 1 *B*. The simplest of the feedback loops is the CheZ module (blue) that responds directly to CheYp concentration. An increase in CheYp concentration leads to the activation of CheZ, which in turn leads to the dephosphorylation of CheYp (Blat et al., 1998). The second feedback loop involves the formation of a complex between CheAs and CheZ. We postulate that an active receptor complex has, on average, a reduced affinity toward CheAs. (The validity of this hypothesis is discussed below.) Thus, an increase in receptor activation renders free CheAs molecules that can associate with CheZ, leading to the formation of CheAs-CheZ complexes. These complexes have a very high CheYp-dephosphorylation activity (Wang and Matsumura, 1996) and therefore have the potential to be potent regulators of CheYp.

Mathematical model

We now formulate the mathematical description of the methylation-independent regulation scheme, i.e., the secondary stage indicated in Fig. 1 *A*. The equations describe the interactions of three variables, CheYp, CheAs-CheZ

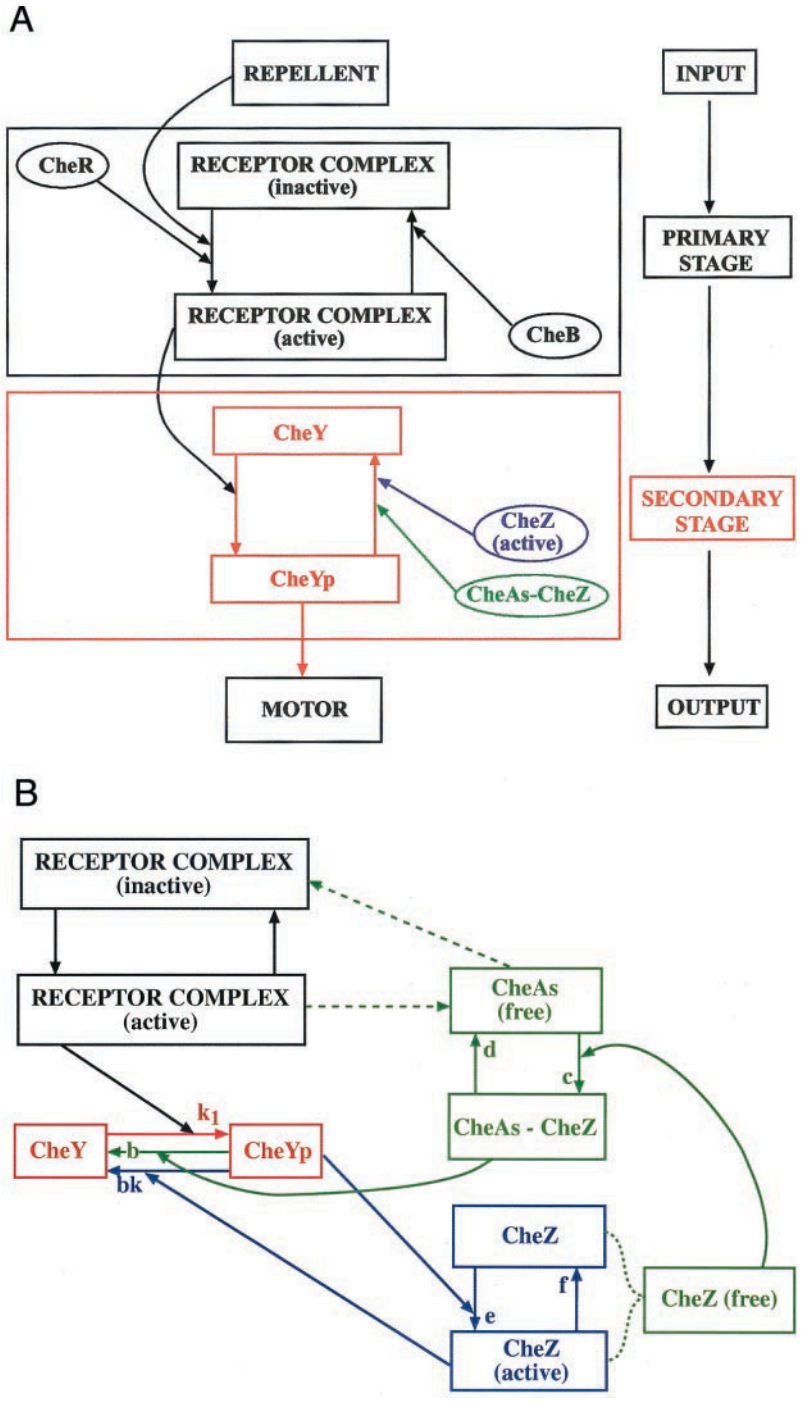

FIGURE 1 (*A*) Two-stage regulation model in bacterial chemotaxis. Repellent (or attractant) serves as input and the bacteria respond to changes in their concentration by modifying the direction of rotation of their motors (the output). It is commonly accepted that the response is determined by the regulation of the methylation state of the receptor complex by the CheR and CheB proteins. This mode of regulation has been the subject of exhaustive modeling efforts. Here we suggest that this mode of regulation serves as the "primary stage" of the regulation, and that its output (i.e., the activation level of the receptor) may serve as the input to a "secondary regulation stage". The secondary regulation stage, which we study theoretically here, involves direct regulation of the concentration of the signal molecule, CheYp, by either CheZ (blue) or CheAs-CheZ (green). (*B*) The components of the secondary stage and their interactions with each other and with components of the primary stage. The secondary stage is composed of two modules, each of which is based on CheYp dephosphorylation (see text). The first module (green) is an activity feedback loop based on the release of CheAs from active receptors. Thus, CheYp, the tumble signal, is both created and destroyed through the activity of the receptor complex and an assistant protein, CheZ. The simpler, second module (blue), includes direct dephosphorylation of CheYp by CheZ. The kinetic coefficients for each biochemical reaction in the network appear near the appropriate arrow.

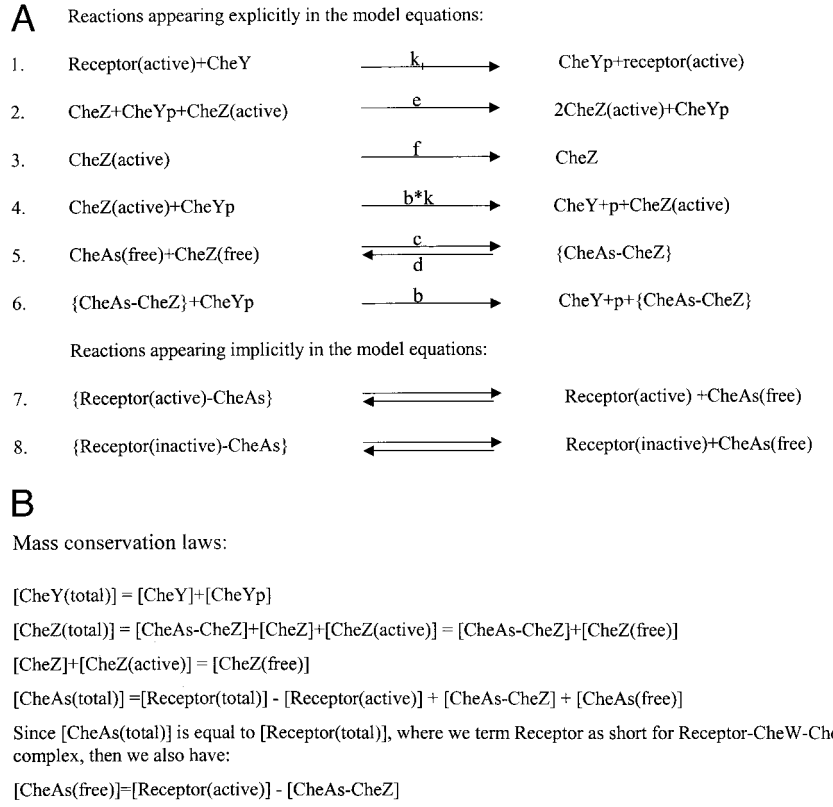

FIGURE 2 The set of kinetic reactions used to derive Eq. 1. (*A*) The model consists of three independent dynamic variables representing the concentrations of CheYp, CheAs-CheZ, and CheZactive. The first six reactions detail the mutual interactions among these variables and are modeled explicitly (Eq. 1). Reactions 7 and 8 are used to assess the concentration of CheAs that has been released from the receptors. Because A is defined as the product of the number of active receptors and their specific activity k_1, A/k_1 is the normalized concentration of active receptor complexes. (*B*) CheY, $CheZ_{free}$ and $CheAs_{free}$ are determined from the three independent dynamic variables CheYp, CheAs-CheZ, and $CheZ_{active}$ and the constants $CheZ_{total}$, $Receptor_{total}$, and $CheY_{total}$ through the mass conservation equations.

complex, and CheZ, whose biochemical kinetic reactions and parameters are given in Fig. 2 *A* and are formalized as

$$\begin{aligned}
\frac{d(CheYp)}{dt} &= A(CheY_{total} - CheYp) \\
&\quad - b \cdot CheYp((CheAs\text{-}CheZ) \\
&\qquad + k \cdot CheZ_{active}), \\
\frac{d(CheAs\text{-}CheZ)}{dt} &= c(A/k_1 - (CheAs\text{-}CheZ)) \\
&\quad \cdot (CheZ_{total} - (CheAs\text{-}CheZ)) \\
&\qquad - d(CheAs\text{-}CheZ), \\
\frac{d(CheZ_{active})}{dt} &= e(CheZ_{active} + \varepsilon)CheYp(CheZ_{free} \\
&\qquad - CheZ_{active}) - f \cdot CheZ_{active}.
\end{aligned} \tag{1}$$

Here $CheY_{total}$ and $CheZ_{total}$ are constants that represent the overall concentration of proteins CheY and CheZ in all their forms (e.g., $CheY_{total}$ = CheY + CheYp) and ϵ is the term that accounts for $CheZ_{active}$-independent activation of CheZ (Blat et al., 1998, and see below). The rate equations were derived in a straightforward manner from the chemical reactions. For example, the rate of CheYp creation is equal to the product of A, the overall receptor activity, and CheY concentration. Its rate of destruction is proportional to the concentration of CheYp and its dephosphorylation agents, CheAs-CheZ and $CheZ_{active}$. More on the parameters and equations may be found in Fig. 2 and Appendix A.

To simplify the analysis of the model, we have made the reasonable approximation that $CheAs_{free}$ concentration (i.e., the CheAs not associated with the receptors or with CheZ) is proportional to the concentration of active receptors, A/k_1. Here, A is the total receptor activity, and k_1 is the receptors' specific activity. A more explicit model of $CheAs_{free}$ concentration would take into account the different possible receptor activity and binding states, such as those shown in Fig. 1 *B*. However, in our model, we simply assume that active receptors lose their affinity to CheAs, which then enters the $CheAs_{free}$ pool, whereas only very few CheAs are dissociated from inactive receptors. Hence, $CheAs_{free}$ con-

centration should be proportional to active receptor concentration A/k_1. This estimate has also been independently justified by a numerical investigation of the relevant reactions (reactions 5, 7, and 8 in Fig. 2 *A*).

Note also that the main purpose of the ϵ term appearing in $CheZ_{active}$ creation rate is to prevent $CheZ_{active}$ from reaching unrealistically low levels or even extinction. The introduction of ϵ could have been avoided had the model incorporated two (or more) activation states of CheZ (Blat et al., 1998). This, however, would add further equations to the model, complicating the analysis with no real gain. Our investigations showed that the explicit allowance of several activation states give qualitatively similar results to the simplified form of the model (unpublished data).

The CheZ and CheAs-CheZ modules

Both simulations and theoretical analysis (Appendix A) show that, for a fixed value of receptor activity A, the model attains a stable steady state. This is seen in Fig. 3 in the period before the stimulus at time $t = 100$. The CheYp level, which represents the swim-to-tumble ratio, is maintained at the steady-state level CheYp = CheYp*, which we will term the reference state.

We are interested in examining how the model responds to a fixed step-wise increase in receptor activity A when initially at the reference state. Intuitively, one might expect that a permanent change in an input parameter should alter the steady-state swim-to-tumble ratio. However, this is not necessarily the case. As Fig. 3, *A*, *B*, and *C* shows, a step-wise increase in receptor activity at $t = 100$ from $A = 0.25$ to 0.5 (*solid lines*), 0.4 (*dashed lines*), and 0.3 (*dotted lines*) triggers phosphorylation of CheY and instantaneously increases CheYp levels. This in turn rapidly activates CheZ, leading to the prompt dephosphorylation and decline of CheYp. At this point, the fast transient dynamics has almost reached completion, leaving CheYp levels to slowly equilibrate to levels near the reference steady-state level, CheYp*. This is facilitated by the action of the CheAs-CheZ complex, the concentration of which has itself slowly been reaching a new steady-state level, corresponding to the newly increased level of receptor activity.

As CheYp levels considerably decline, the activity of CheZ, which reacts to the level of CheYp, is also reduced, and the steady state of CheYp depends chiefly on the conflict between the phosphorylating receptor activity and the dephosphorylating CheAs-CheZ activity. The CheYp steady state finally achieved depends on the degree of adaptiveness of the model. For a system with exact adaptation, the steady state returns to the reference (i.e., pre-perturbation) level CheYp*. (An 80% precision of adaptation to an attractant, for example, would shift the new steady state to 0.8 CheYp*.). The CheAs-CheZ-driven adaptation as presented here allows for >98% precision of adaptiveness to a two-fold increase in receptor activity (Fig. 3 *A*, *solid line*), and over 99% for the two smaller changes (*dashed* and *dotted lines*). To summarize, the rapidity of the response hinges on the CheYp-induced activation of CheZ dephosphorylation, whereas the steady-state CheYp level finally reached is determined by the CheAs-CheZ dephosphorylation complex. Note that CheAs-CheZ complex formation may take up to a few minutes (Gegner et al., 1992). Therefore, the time required for exact methylation-independent adaptation may also be on the time-scale of minutes (Stock et al., 1985). Note that we are only interested here in the methylation-independent adaptation, not response or chemotactic ability, which is poor in CheR/CheB mutants.

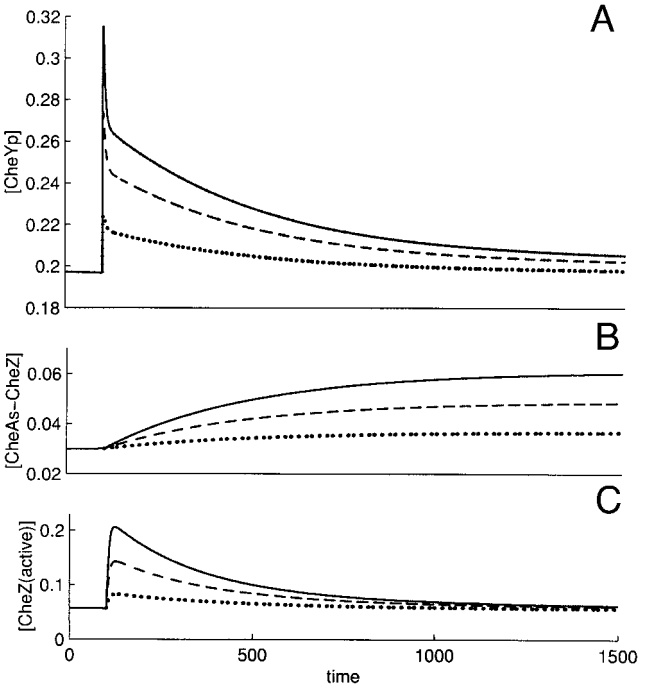

FIGURE 3 Rapidity and exactness. Model simulations (Eq. 2) of CheZ- and CheAs-CheZ-driven adaptation to various changes in activity levels, A. At time $t = 100$, activity $A = 0.25$ was elevated to 0.5 (*solid lines*), 0.4 (*dashed lines*) and 0.3 (*dotted lines*). (*A*) As a response, model CheYp levels were immediately elevated to ~150%, 135%, and 115% of their prestimulus levels, respectively, and then adapted in two stages: first, a rapid decline mediated by CheZ activation and finally returning very close to their original quiescent steady-state level by the action of the CheAs-CheZ complex (max. 2% deviation). Note that this is only one stage of two in our proposed mechanism, and, according to our theory, each stage by itself does not have to be 100% accurate. (*B*) Although CheAs-CheZ levels responded to the change in activity A, neither showed any signs of adaptation and, in contrast, were attracted to steady-states significantly different from their prestimulus level. (*C*) CheZ levels rapidly increase in response to an increase in CheYp levels. However, as CheYp returns to its prestimulus level, CheZ follows and also demonstrates exact adaptation (associated with CheYp dynamics).

An explanation for the model's high adaptiveness is provided in the following mathematical analysis. First, the

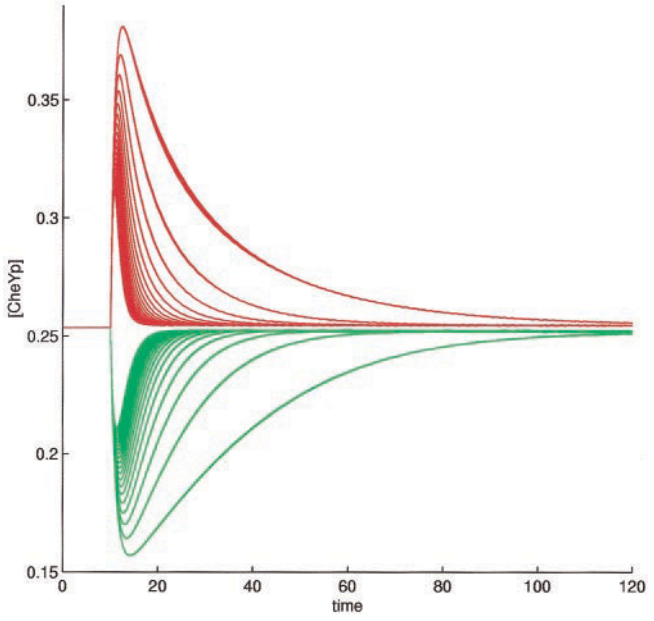

FIGURE 4 Robustness: CheYp versus time for various choices of parameters. At time $t = 10$, activity A was doubled from 0.25 to 0.5 (addition of repellent, red convex lines) and symmetrically lowered to 0.125 (an addition of attractant, green concave lines). Simulations were repeated after systematically changing parameters (c, d, and f), by up to two orders of magnitude; the steady state was robust to such changes. Parameters used as described in Appendix A.

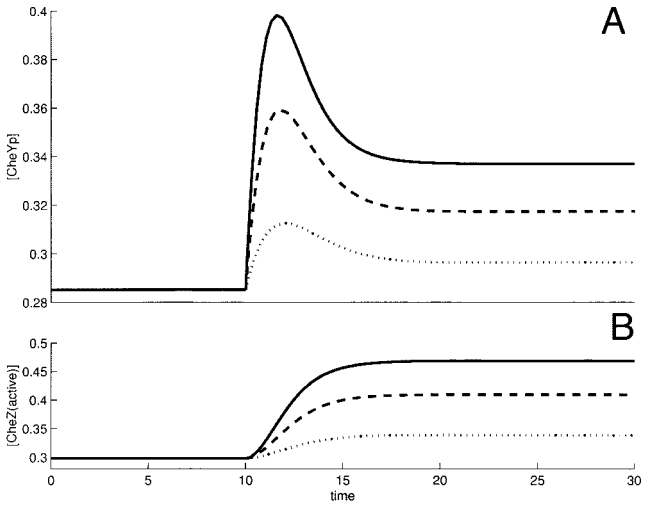

FIGURE 5 Model simulations of CheZ-driven adaptation to various changes in activity levels (Eq. 4). At time $t = 10$ receptor activity was increased from its resting value of $A = 0.25$ to $A = 0.3$ (*dotted lines*), $A = 0.4$ (*dashed lines*) and $A = 0.5$ (*solid lines*). (*A*) The transient dynamics ($10 < t < 30$), consisting of a large increase and a sharp decrease in CheYp level, is noticeable. This is indicative of the capacity of the CheZ module to provide a rapid signal regulation. However, the long-term steady-state level of CheYp is significantly shifted from its reference level, CheYp*. For example, for a 100% increase in receptor activity A, CheYp deviates by 18%. (*B*) $CheZ_{active}$ levels rise sharply and remain at a new steady-state value significantly higher then the prestimulus $CheZ^*_{active}$.

number of model parameters in Eq. 1 may be reduced by using dimensionless variables (see Appendix A):

$$\frac{dx}{dt} = A(1 - x) - bx(y + kz),$$

$$\frac{dy}{dt} = c(A/k_1 - y)(1 - y) - dy,$$

$$\frac{dz}{dt} = e(z + \varepsilon)x(1 - y - z) - fz, \qquad (2)$$

where x = CheYp, y = CheAs-CheZ complex, and z = $CheZ_{active}$. Without loss of generality (see Appendices B and C), we first consider the simplified case when $\epsilon = d = 0$. For the parameter ranges of interest, the model has one stable steady state (see Appendix A),

$$x^* = \frac{k_1}{k_1 + b}, \quad y^* = A/k_1, \quad z^* = 0. \qquad (3)$$

It is easy to see that the steady state is perfectly adaptive, because, here, the CheYp* steady-state level ($x^* = k_1/(k_1 + b)$) is clearly unaffected and independent of changes in receptor activity input A. This is a surprising result, given that the receptor activity A is a prominent flux in the rate equation for CheYp (i.e., dx/dt) in Eq. 2. In Appendix B, it is shown that, for realistic nonzero parameter choices of d, the steady-state x^* becomes a function of A, i.e., $x^* = F(A)$. Now for a small change in receptor activity A, (δA), the resulting change in the CheYp steady-state level (δx^*) depends largely on $F'(A)$

$$\delta x^* \cong F'(A)\delta A.$$

As Appendix B makes clear, the CheYp steady-state level remains largely insensitive to any changes in receptor activity A because $F'(A)$ is always relatively small. That is, despite significant long-term or permanent changes in the receptor activity input, the CheYp steady state changes very little. This remarkable adaptiveness is achieved by the coupling of CheAs dissociation to the receptor activity. Not only does the phosphorylation/dephosphorylation regulatory level in the model demonstrate adaptiveness to changes in receptor activity input, but also this form of regulation is robust to changes in parameters (of several orders of magnitude), such as the kinetic rate constants and protein concentration. Figure 4 makes clear that, although the transient dynamics of the model differ for attractants and repellants and for various parameter ranges, the steady-state solution for CheYp level remains almost unchanged to major parameter shifts (the parameters c, d, and f, Fig. 2), indicating robustness of adaptation in the same manner as in Barkai and Leibler (1997).

The CheZ module

The key assumption behind the analysis so far is that CheAs dissociates preferentially from active receptors (and associates with nonactive receptors). Here, we examine whether realistic adaptation is maintained upon removal of the CheAs pathway (green module; Fig. 1 *B*) from the model. By setting the initial concentration of the CheAs-CheZ complex and its rate of change to zero in Eq. 1, we obtain the reduced system,

$$\frac{\mathrm{d}(\mathrm{CheYp})}{\mathrm{d}t} = A(\mathrm{CheY}_{\mathrm{total}} - \mathrm{CheYp}) - b \cdot \mathrm{CheYp}(k \cdot \mathrm{CheZ}_{\mathrm{active}}),$$

$$\frac{\mathrm{d}(\mathrm{CheZ}_{\mathrm{active}})}{\mathrm{d}t} = e(\mathrm{CheZ}_{\mathrm{active}} + \varepsilon)\mathrm{CheYp}(\mathrm{CheZ}_{\mathrm{free}} - \mathrm{CheZ}_{\mathrm{active}}) - f \cdot \mathrm{CheZ}_{\mathrm{active}}. \quad (4)$$

We repeated our previous analyses on the reduced system and obtained the numerical simulation results presented in Fig. 5. At time $t = 10$, the system is significantly perturbed, with receptor activity jumping from $A = 0.25$ to $A = 0.3$, $A = 0.4$, and $A = 0.5$, as before. CheYp levels rise immediately following the increase in receptor activity, decrease, and then approach a new equilibrium level. The errors in adaptation are 3%, 13%, and 18%, respectively. That is, in response to small permanent changes in receptor activity, CheZ alone can regulate CheYp levels on the fast time scale required for chemotactic behavior with a >96% precision. Note that the adaptation time is on very short timescale when CheAs is removed from the system. However, there are a couple of difficulties in eliminating CheAs from the system and basing the methylation-independent adaptation solely on CheZ activity. First, as can be seen in Fig. 5, the adaptation is far less exact without the presence of CheAs and could not account for the actual adaptation observed. Furthermore, the reported methylation-independent adaptation time is of the order of minutes (Stock et al., 1985), far too slow for the rapid CheZ activation.

It is evident from the analysis above that neither the CheZ (Fig. 5) nor the CheAs-CheZ (Fig. 3) theoretical modules can alone attain the necessary qualities essential for chemotactic behavior. For instance, CheZ facilitates a rapid response but, by itself, is not highly accurate (Fig. 5), whereas the putative CheAs-CheZ module is accurate but lacks the rapidity of CheZ activation. Moreover, Fig. 3 demonstrates that, even the full secondary regulatory stage, composed of both modules, does not produce 100% exactness of adaptiveness. Likewise, the primary regulatory stage, that is, the methylation-dependent mechanism, also does not appear to be accurate enough by itself given the bacterial motor's prominent sensitivity to CheYp levels (e.g., Morton-Firth et al., 1999). It is noteworthy that many interactions that may take place in the busy cellular environment were ignored in the idealized theoretical studies provided here and elsewhere (Asakura and Honda, 1984; Bray et al., 1993; Hauri and Ross, 1995; Barkai and Leibler, 1997; Spiro et al., 1997). Thus, in reality, the performance of both regulatory stages is probably even less accurate than that of the model system. However, in the next section, we will demonstrate that the manner in which these regulatory units are connected ensures high adaptiveness and robustness, despite the inadequacy of each of them alone.

MULTI-STAGE REGULATION

In the bacterial chemotactic system, both methylation/demethylation and phosphorylation/dephosphorylation processes may act as independent regulators (Fig. 1 *A*), and both are likely to have some degree of imprecision in their adaptiveness. Yet, multistage regulation operates so that the adaptation achieved by coupling the two systems together is far more exact than the adaptation of the individual components. Multistage regulation is based on the principle that any imprecision introduced in the first stage can be significantly attenuated by another linearly connected "downstream" regulator—composed of the CheAs and CheZ participants in this case. The attenuation is, in fact, multiplicative—the more stages in the system, the less the error introduced by the input perturbation can be transmitted through the chain of regulators.

The underlying mechanism of multistage regulation may be understood as follows. Consider first a single regulatory unit examined at some arbitrary reference state in which the regulator maintains a particular variable X at a constant stable steady-state level $X^* = X^*_r$, for a fixed reference input level. In a perfectly adaptive system, the steady-state level would remain fixed to $X^* = X^*_r$ notwithstanding changes in the regulator's input from the reference level $A = A_r$.

However, if the system were not perfectly adaptive, the steady-state level X^* would, in general, be some function of the input level, $X^* = F(A)$. To gain an idea of how adaptive a system might be to a change in input level, we examine the steady-state dynamics about the reference state using a Taylor expansion,

$$X^*(A_r + \Delta A) \cong X^*_r + F'(A_r)\Delta A,$$

or

$$\Delta X^* \cong F'(A_r)\Delta A. \quad (5)$$

Here $F'(A_r) = \mathrm{d}F/\mathrm{d}A$ is the derivative evaluated at the reference state $A = A_r$. A change in input level to $A = A_r + \Delta A$, thus shifts the steady-state level to $X^* = X^*_r + \Delta X^*$. Note that the smaller ΔX^* is, the more precise is the adap-

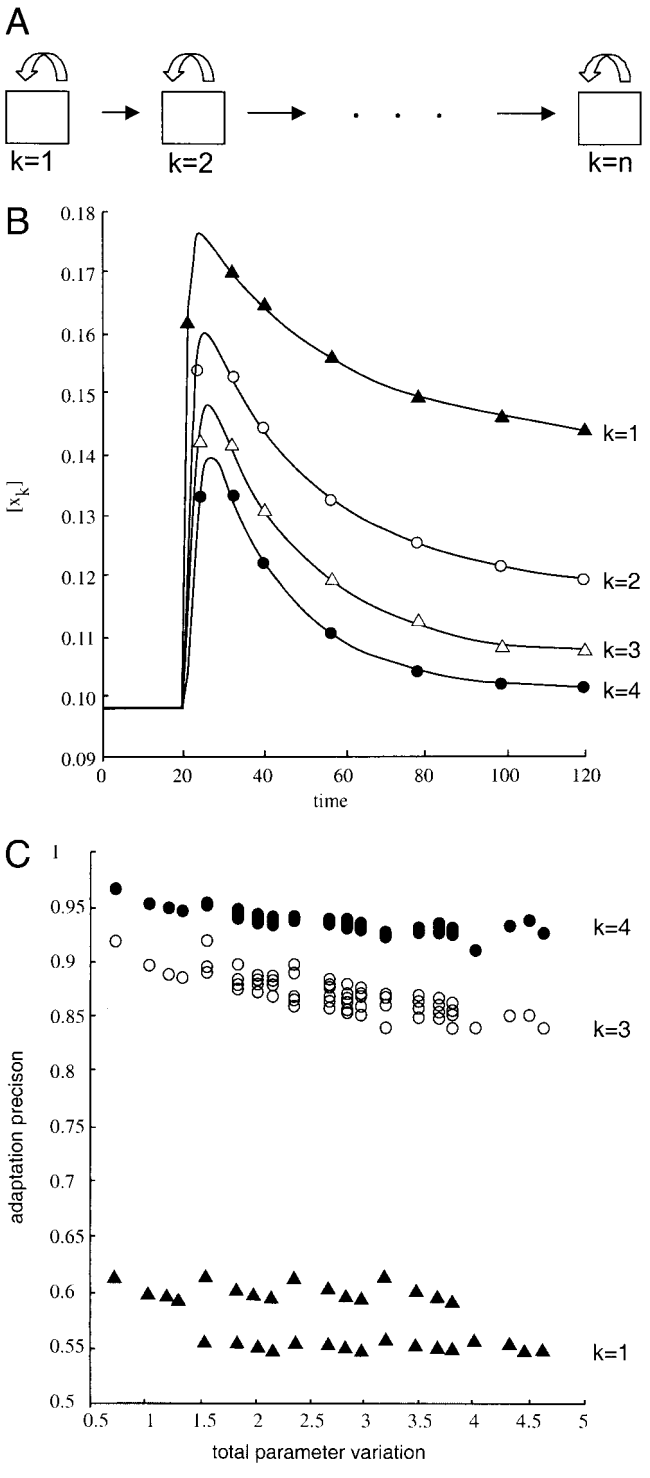

FIGURE 6 (*A*) Multistage regulation may be understood by considering a chain of n identical regulatory units connected so that the output of the k'th unit (X_k) feeds into the input of the $(k + 1)'$th unit. The external input of the first regulator in the chain is activity level A. The results presented in B and C were obtained by numerical simulations of the hypothetical biochemical regulatory unit in Eq. D1 (Appendix D). (*B*) Exact adaptation. The quiescent activity level is set to $A = 0.1$ and the steady-states of four such units are $X_k^* \sim 0.1$. At $t = 20$, activity changes to $A = 0.2$, causing immediate excitation of all X_k. Now, however, X_1 (*filled triangles*) equilibriates to $X_1^* \sim 0.15$, some 50% higher than its quiescent level, indicating that each unit has low precision of adaptation. Nevertheless, the final unit (*filled circles*) attains a steady state of $X_4^* < 0.104$, some 4% higher than its quiescent level, indicating the very effective operation of multistage regulation. (*C*) Robustness. A plot of the precision of adaptation (P), defined as the ratio of X_k at time $t = 20$ to X_k at $t = 120$, versus total parameter variation (V), defined as $V = \Sigma_{i=1}^{N} \log(a_i/a_f)$ (Barkai and Leibler; 1997, where a_f and a_i are the biochemical parameters of the altered and unaltered systems, respectively. When varying parameters widely, the exactness of each unit is impaired, as clearly seen for $k = 1$ (*filled triangles*) where $p < 0.65$. However, when three of the regulatory units are linearly connected to each other, $k = 3$ (*open circles*), the system is more resistant to parameter variations, and, for four serially connected units, $k = 4$ (*filled circles*), the system has very high precision of adaptation ($p > 0.92$).

tation. Perfect (100%) adaptation implies that $\Delta X^* = 0$ and thus $F'(A_r) = 0$, whereas a well-adapted system is characterized by $F'(A_r) \ll 1$.

Consider now a chain of two such regulators R_1 and R_2 connected in series (e.g., the methylation-dependent and -independent levels of Fig. 1). The output (X) of R_1 is connected to the input of R_2, whereas the input of the coupled system is still A. At an arbitrary reference state with input A_r, the regulators R_1 and R_2 attempt to maintain their respective output variables X and Y at the steady-state values $X_r^* = F_1(A_r)$ and $Y_r^* = F_2(X_r^*)$. As before, the adaptation properties of the individual regulators are governed by $F_1'(A_r)$ and $F_2'(X_r^*)$; the smaller the absolute value of the derivative, the more adaptive is the regulator. Under these conditions, if the input changes from the reference state to $A = A_r + \Delta A$, the steady state of the end regulator R_2 will shift from Y_r^* by an amount,

$$\Delta Y^* \cong F_2'(X_r^*)F_1'(Ar)\Delta A. \tag{6}$$

Thus, the adaptiveness of the full system, which now consists of two serially connected regulators, is governed by the product $F_2'(X_r^*)\ F_1'(A_r)$. Assuming that each single system is reasonably well adapted ($F_1'(A_r) \ll 1,\ F_2'(X_r^*) \ll 1$) then the adaptiveness of the full system is far greater than either individual system alone because the product $F_1'(A_r)F_2'(X_r^*)$, and thus ΔY^*, is now almost negligible.

The scheme can be generalized for a chain of n-leveled multistage regulators, so that the final adaptation error is proportional to,

$$\Delta Y^* \cong \prod_{i=1}^{n} F_i' \Delta A, \tag{7}$$

where the derivatives F_i' are evaluated at the system's reference steady state. In this way, one sees that the errors in adaptation can attenuate considerably with every new regulatory step. Once this concept is noted, it is possible to construct precise and robust models even from seemingly simple regulatory units, each having low accuracy, as

clearly demonstrated in Fig. 6. The figure shows how a set of four consecutive identical regulatory units, each of which is inaccurate and sensitive to parameters alone, produces a highly accurate (Fig. 6 *B*) and robust (Fig. 6 C) system.

DISCUSSION

We introduced two related new ideas, both of which deserve further consideration. First, we suggested that CheZ and CheAs-CheZ may serve in two parallel, negative feedback loops that down-regulate the level of CheYp (Fig. 1, *secondary stage*). Our modeling study predicts that the methylation-independent mechanism by itself provides an almost exact adaptation for small ligand concentrations, an adaptation that becomes increasingly impaired for larger changes in receptor activity (see Appendix B), in accord with experimental data (Stock et al., 1985). CheZ-mediated deactivation of CheYp may facilitate rapid adaptation, but only to small changes in receptor activity. Moreover, our studies suggested a solution to the puzzling role of CheAs (Sanatinia et al., 1995), placing it as an essential component of a down-stream regulatory unit controlling the level of CheYp. This suggestion calls for experimental verification; for example, to verify the specific mechanism we suggested, it should be tested whether CheAs indeed has a reduced affinity toward active receptors in vivo.

Our simulations and analysis (Appendix B) suggested that the down-stream regulatory unit is highly exact (Fig. 3 *A*) and robust to changes in protein concentration and kinetic rate constants (Fig. 4) in its ability to maintain the level of CheYp*. However, the motor is extremely sensitive to changes in the concentration of CheYp (Cluzel et al., 2000), implying that the exactness provided by either the methylation-dependent or -independent regulatory levels by themselves may not suffice to account for the experimentally observed stable chemotaxis behavior. Therefore, we further suggested that the new level of regulation, involving CheZ and CheAs-CheZ complexes, adds to the previously documented level based on methylation-dependent regulation, and to the newly found level involving the reduced affinity of methylated receptors for their ligands (Li and Weis, 2000). The linear manner in which these regulatory units are connected (Fig. 1 *A*) produces a robust and exact system. Again, this suggestion calls for an experimental proof, i.e., the experimental equivalent of Fig. 6.

The most problematic issue in applying chemical kinetic models to biological systems is that the values of many of the kinetic rate constants are unknown. This is not a major problem with regard to the adaptation of CheYp in the model, because the exactness of adaptation is inherently robust and mostly insensitive to the choice of parameters (Fig. 4). Moreover, we demonstrated an exact and robust adaptation in multistage regulation in general (Fig. 6 *C*). Thus, CheYp's return to steady state, which is regulated both by the primary and secondary stages of Fig. 1, should be highly insensitive to the choice of parameters.

However, the transient dynamics of CheYp in our model strongly depend on the choice of the kinetic rate constants. Activation and deactivation of CheZ takes place within tenths of a second (Blat et al., 1998) and the corresponding kinetic rate constants were chosen to reproduce the rapid dynamics (see Figs. 3 and 5) observed for CheZ activation and essential for efficient chemotactic behavior (Segall et al., 1986). There are no experimental data on the transient dynamics of formation and dissociation of the CheAs-CheZ complex, and so we had to rely on estimates. On average, receptor complex assembly from its basic subunits (including CheAs) takes about 7 ± 2 min (Gegner et al., 1992). It is noteworthy that the 7 ± 2-min value given should probably be regarded as an upper bound for CheAs-CheZ complex formation time because the reduction of dimensionality imposed by the membrane enhances the rate of receptor complex formation in vivo (Liu et al., 1997). Nevertheless, taking this value as an estimate for CheAs-CheZ complex formation time implies that CheAs is not a primary force in rapid adaptation to small changes in the chemical environment. Rather, it is probably involved in the slow restoration of CheYp to its steady-state level CheYp* in response to large environmental changes.

The model proposed here for the regulation of the chemotactic behavior of bacteria is more realistic than models solely based on methylation-dependent regulation, in that it explains experimental data not accounted for in previous models; the most obvious example being the model's ability to account for methylation-independent adaptation. Also, being proximate to the motor, the down-stream regulation proposed here is likely to have exquisite control not only over the adaptation precision, but also over the swim-to-tumble ratio itself. Because it is the adaptation, and not the steady-state activity level that is robust in previous models (Barkai and Leibler, 1997), the steady-state level of CheYp would be expected to be greatly affected by changes in CheZ concentration or the receptor steady-state activity. Such major changes would result in frequent occurrences of individual bacteria locked into either a swim or a tumble mode, as the CheYp steady-state level is either too high or too low, for effective chemotactic behavior (Cluzel et al., 2000). The model we describe overcomes this difficulty because it offers both a direct regulation over CheYp level and a mechanism that maintains a CheYp level that is not much affected by varying the number of receptors active at steady-state (Barkai and Leibler, 1997).

The model also sheds light as to why CheYp steady-state level is not affected too strongly by variation in CheZ level (Huang and Stewart, 1993; Sanna and Simon, 1996). This result comes about because it is the steady-state CheAs-CheZ concentration that serves as the primary control over CheYp concentration and not $CheZ_{active}$, thus variations in

CheZ have a reduced effect in the presence of CheAs (whether CheAs dissociates from active receptors or not).

Despite these encouraging results, the model given here is only a simplification of the actual processes taking place. For example, the total receptor activity is the sum of many receptors flicking conformations between active and inactive states (Morton-Firth et al., 1999), both when they are and when they are not bound to CheAs. In our model, however, it is the active/inactive receptor populations that are modeled, rather than the individual receptors. Thus, in determining $\mathrm{CheAs}_{\mathrm{free}}$ concentration it does not matter whether a specific receptor has flicked between the active and inactive conformations. The relevant issue for our modeling effort is that an increase in active receptor concentration would result in the release of more CheAs from the total receptor population. Changes in the receptor-flicking pattern are neglected. The model also neglects the effect of clustering of the chemotaxis receptors at the bacteria's poles, a well-documented phenomenon, which may play a role in the chemotactic network (Barkai and Leibler, 1998; Bray et al., 1998; Lybarger and Maddock, 1999). Finally, recent evidence indicates that CheY and CheZ co-localize with receptor complexes in vivo (Sourjik and Berg, 2000). Co-localization is likely to result in higher values for the kinetic constants, but, because our model is robust to such changes, and co-localization will not affect the results qualitatively. Obviously, it may be of fundamental importance in other aspects of chemotaxis.

While the suggested idea of multistage regulation is interesting in the context of the bacterial chemotaxis system described here, it may be applicable to other cellular networks as well. For example, the highly reliable protein transport between the endoplasmic reticulum (ER) and the Golgi apparatus (Ellgaard et al., 1999) uses at least two independent stages of regulation. The cell marks proteins destined to leave the ER with a specific mark, and ER resident proteins with a different mark (Fullekrug and Nilsson, 1999). Hence, when, because of the inherent inexactness of biochemical machinery, an ER resident protein is exported out of the ER, a second mechanism recognizes this error (according to the mark on the protein) and the protein is transported back in, thereby attenuating the error rate. This setting has led to the protein transport "distillation hypothesis" (Fullekrug and Nilsson, 1999), which is a special, simple case of the multistage regulation principle. However, multistage regulation may be constructed out of far more complex regulation modules, each having multiple regulation layers by itself, as is the case in cellular quality control during protein translation (Ibba and Soll, 1999). Viewing biochemical networks as independent yet highly connected smaller networks may thus prove to be an important tool in the analytical analysis of large regulated biochemical processes, as in the construction and implementation of artificial biochemical networks in the highly complex environment of the human body.

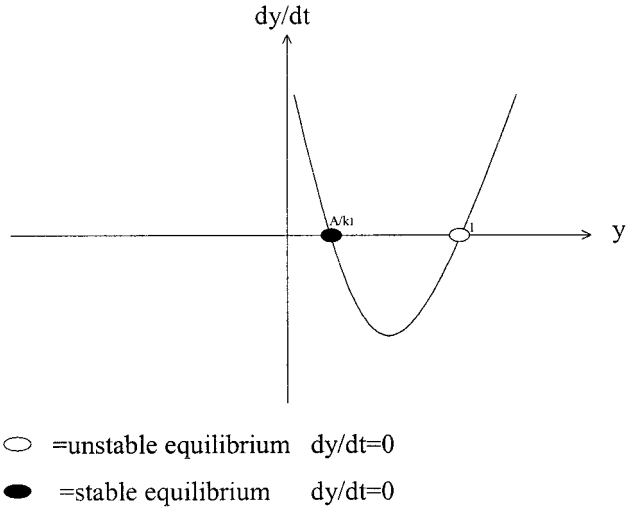

FIGURE A1

APPENDIX A: THE MODEL

The set of equations in Eq.1 was derived from the biochemical reactions and mass conservation laws of Fig. 2. To simplify notation, let x = CheYp, y = CheAs-CheZ complex, and z = $\mathrm{CheZ}_{\mathrm{active}}$. Eq. 1, then, reads:

$$\frac{\mathrm{d}x}{\mathrm{d}t} = A(\mathrm{CheY}_{\mathrm{total}} - x) - bx(y + kz)$$

$$\frac{\mathrm{d}y}{\mathrm{d}t} = c(A/k_1 - y)(\mathrm{CheZ}_{\mathrm{total}} - y) - dy$$

$$\frac{\mathrm{d}z}{\mathrm{d}t} = e(z + \varepsilon)x(\mathrm{CheZ}_{\mathrm{total}} - y - z) - fz$$

The model can be simplified using the dimensionless variables:

$$x' = \frac{x}{\mathrm{CheYp}_{\mathrm{total}}}; \quad y' = \frac{y}{\mathrm{CheZ}_{\mathrm{total}}}; \quad z' = \frac{z}{\mathrm{CheZ}_{\mathrm{total}}}$$

with

$$e' = [e \cdot \mathrm{CheY}_{\mathrm{total}} \cdot \mathrm{CheZ}_{\mathrm{total}}];$$

$$A' = A[e \cdot \mathrm{CheY}_{\mathrm{total}} \cdot \mathrm{CheZ}_{\mathrm{total}}];$$

$$b' = b \cdot \mathrm{CheZ}_{\mathrm{total}}/[e \cdot \mathrm{CheY}_{\mathrm{total}} \cdot \mathrm{CheZ}_{\mathrm{total}}];$$

$$c' = c \cdot \mathrm{CheZ}_{\mathrm{total}}/[e \cdot \mathrm{CheY}_{\mathrm{total}} \cdot \mathrm{CheZ}_{\mathrm{total}}];$$

$$d' = d/[e \cdot \mathrm{CheY}_{\mathrm{total}} \cdot \mathrm{CheZ}_{\mathrm{total}}];$$

$$f' = f/[e \cdot \mathrm{CheY}_{\mathrm{total}} \cdot \mathrm{CheZ}_{\mathrm{total}}];$$

$$k_1' = k_1/[e \cdot \mathrm{CheZ}_{\mathrm{total}} \cdot \mathit{CheY}_{\mathrm{total}} \cdot \mathrm{CheZ}_{\mathrm{total}}];$$

Eq. 2 was derived from the set of equations above by rescaling time to $t' = e'^{*}t$ and omitting primes.

Choice of parameters

The parameter e in Eq. 1 is constant and scales out after rescaling time (see Eq. 2). By taking $c = 0.0025$ and $d = 0.00005$ (c:d = 50:1) the CheAs-CheZ is rendered a slowly forming, stable complex (as reported in Wang and Matsumura, 1996). $b = 30$, chosen to keep $x^* = k_1/(k_1 + b)$ (see below) in the approximate range $\frac{1}{3} > x^* > \frac{1}{10}$ (Alon et al., 1998). $k = \frac{1}{14}$ (Wang and Matsumura, 1996). $f = 0.1$—an arbitrary choice ensuring that E_1, the steady state relevant in this discussion, would be the stable steady state. Note that, for smaller choices of f, E_2 (another equilibrium, see below) may be stable and E_1, in turn, unstable. However, qualitatively, the results remain unchanged (data not shown) when the adaptiveness of E_2 is examined. We tested k_1 values in the range one to ten, and found that, qualitatively, the results were the same regardless of the choice of k_1. This observation was analytically verified (Appendix B).

Steady states

The basic model equations, Eq. 2, possess the following four different steady states found by setting $dx/dt = dy/dt = dz/dt = 0$:

$$E_1: \quad x^* = \frac{k_1}{k_1 + b}, \qquad y^* = \frac{A}{k_1}, \quad z^* = 0$$

$$E_2: \quad x^* = \frac{A + bkf}{A + b(A/k_1 + k - Ak/k_1)},$$

$$y^* = \frac{A}{k_1}, \quad z^* = 1 - \frac{A}{k_1} - \frac{f}{x^*}$$

$$E_3: \quad x^* = \frac{A}{A + b}, \qquad y^* = 1, \quad z^* = 0$$

$$E_4: \quad x^* = \frac{A + bkf}{A + b}, \qquad y^* = 1, \quad z^* = -\frac{f}{x^*} \tag{A1}$$

Stability

To examine the stability of the steady-states, we first note that, for the equation $dy/dt = f(y)$ in Eq. 2, namely,

$$\frac{dy}{dt} = f(y) = c(A/k_1 - y)(1 - y) - dy, \tag{A2}$$

$f(y)$ is independent of the other variables x and z. Hence, y reaches steady state (y^*) in a manner that is completely independent of x and z. Inspection of Eq. A2, with $d = 0$, reveals that y has two steady states $y^* = A/k_1$ and $y^* = 1$. A standard phase plane analysis of $dy/dt = f(y)$ reveals that the steady state $y^* = \mathrm{Min}\{A/k_1, 1\}$ is locally stable (see Fig. A1). Equivalently, in terms of the unscaled variables in Eq. 1, the steady state CheAs-CheZ* = $\mathrm{Min}(A/k_1, \mathrm{CheZ}_{\mathrm{total}})$. However, it is known from the literature that $A/k_1 < \mathrm{CheZ}_{\mathrm{total}}$ (Stock and Surrete, 1996). It follows that $y^* = A/k_1$ is the only stable steady-state. The steady-states E_3 and E_4 are unstable and may therefore be disregarded for our purposes here.

Based on the knowledge that y will always be attracted to its steady state $y^* = A/k_1$, we now proceed to determine the local stability of the full system's steady state (x^*, y^*, z^*) by studying the first and last equalities of Eq. 2:

$$\frac{dx}{dt} = f(x, z) = A(1 - x) - bx(y^* + kz)$$

$$\frac{dz}{dt} = g(x, z) = xz(1 - y^* - z) - fz$$

with Jacobian,

$$J = \begin{bmatrix} \frac{\partial f}{\partial x} & \frac{\partial f}{\partial z} \\ \frac{\partial g}{\partial x} & \frac{\partial g}{\partial z} \end{bmatrix}$$

$$= \begin{bmatrix} A - b(y^* + kz) & -bxk \\ z(1 - y^* - z) & x - xy^* - 2xz - f \end{bmatrix}. \tag{A3}$$

For E_1 (see Eq. A1), the eigenvalues of the Jacobian (Eq. A3), evaluated at the steady state are

$$\lambda_1 = -(A + by^*); \quad \lambda_2 = x^*(1 - y^*) - f.$$

Because $\lambda_1 < 0$, local stability is ensured if $\lambda_2 < 0$, so that both eigenvalues are negative,

$$f > x^*(1 - y^*). \tag{A4}$$

Hence, as long as the above condition on the parameter f is kept, the steady state E_1 is locally stable. A similar argument shows that E_2 is unstable under these conditions.

APPENDIX B: EXACT ADAPTATION

Recall that, in the main text, exactness of adaptiveness was quantified by $F'(A)$, where the CheYp steady state $x^* = F(A)$. For $\epsilon = d = 0$, the (locally stable) steady state of interest is

$$E_1: \quad x^* = \frac{k_1}{k_1 + b}, \qquad y^* = \frac{A}{k_1}, \quad z^* = 0.$$

Because x^* is completely independent of A (i.e., $F'(A) = 0$), the system has exact adaptiveness. However, once the assumption that $d = 0$ is relaxed, the steady-state value x^* is a function of A, i.e., $x^* = F(A)$. We now determine $F'(A)$ assuming $d \ll c$, because this signifies biologically that the CheAs-CheZ complex is a stable one. Evidence for this may be found in, e.g., Wang and Matsumura (1996). First, from Eq. A2, it is possible to approximate $y^* = A/k_1 + \delta y^*$, where δy^* is the component deriving from the small nonzero parameter d. A calculation shows that

$$\delta y^* = \frac{Ad}{k_1 c(1 - A/k_1)}. \tag{B1}$$

The change in the CheYp steady-state x^* is now approximated by

solving $dx/dt = 0$ from Eq. 2 but now substituting $y^* = A/k_1 + \delta y^*$. The resulting expression is

$$\frac{\delta x^*}{\delta A} = F'(A) = \frac{bc\delta y^*}{(1 + b(1 + \delta y^*))^2(c(A/k_1 - 1) - d)}.$$

Finally, for realistic A/k_1 values (i.e., with $A/k_1 < 0.5$ $CheZ_{total}$ in the unscaled variables of Eq. 1), the expression simplifies to

$$F'(A) < \frac{4d}{bc} \ll 1,$$

with $d \ll c$ and $b = 10$, as in the model simulations. Recall that adaptation may be gauged by examining

$$\delta x^* \cong F'(A)\delta A.$$

We have thus shown that the deviation from exact adaptation is very small for small changes in A when the parameter d is nonzero. Within our typical parameter range $F'(A) < 1/50$ so that δx^* would be smaller than $1/50$ leading to a minimum of some 98% adaptation. This theoretical prediction is in good agreement with numerical results.

The result breaks down, to some extent, if the receptor activity A is relatively large, which, in turn, can lead to imprecision in the adaptation. However, this is also in accord with experimental findings (Stock et al., 1985), because methylation-independent adaptation is more effective when ligand changes are small. We believe that this difficulty is resolved by the proposed multistage regulation mechanism.

APPENDIX C: THE SIGNIFICANCE OF ϵ IN THE MODEL

Recall that the (locally stable) steady state of interest is

$$E_1: \quad x^* = \frac{k_1}{k_1 + b}, \qquad y^* = \frac{A}{k_1}, \quad z^* = 0.$$

However, this has the unrealistic disadvantage that, when $CheZ_{active}$ reaches its steady-state level $z^* = 0$, CheZ is completely lost from the system and can never be restored. To overcome this, we have introduced the term ϵ in Eqs. 1, 2, and 4, which perturbs the steady-state z^* to some small positive quantity $z^* \ll 1$ and has little effect on x^* and y^*. There is also a biological motivation for introducing the term ϵ. Experiments have shown (Blat et al., 1998) that CheZ's activation is cooperative (more CheZ implies more activation), yet it is very plausible that a CheZ molecule can undergo activation even with no active CheZ present.

APPENDIX D: MULTI-STAGE MODEL

In constructing the system used for Fig. 6, *B* and *C*, we connected four trivial feedback loops (X_k, Y_k), where the output of X_k served as the input of X_{k+1}. Each feedback loop, or submodel, is constructed based on the following set of kinetic equations (NA = nonactive, A = active):

$$X_k(\mathrm{NA}) \xrightarrow{\alpha X_{k-1}} X_k(\mathrm{A})$$

$$X_k(A) + Y_k(NA) \xrightarrow{\gamma} X_k(A) + Y_k(A)$$

$$X_k(A) + Y_k(A) \xrightarrow{\beta} X_k(NA) + Y_k(A)$$

$$Y_k(A) \xrightarrow{\delta} Y_k(NA),$$

which leads to the mathematical model,

$$\frac{dX_k(A)}{dt} = \alpha X_{k-1}(A)(1 - X_k(A)) - \beta Y_k(A)X_k(A)$$

$$\frac{dY_k}{dt} = \gamma X_k(A)(1 - Y_k(A)) - \delta Y_k(A)$$

$$k = 1, 2, \ldots, n \quad \text{(D1)}$$

where the variables X_k activates Y_k while Y_k deactivates X_k, thus forming a negative feedback loop.

Figure 6 was generated by numerically solving Eq. D1. Parameters used were: $\alpha = 1$; $\beta = 10$; $\gamma = 0.01$; $\delta = 0.01$; δ and γ were chosen to be small to ensure initial model excitation. Plot parameters were chosen so that all prestimulus steady states $x_1^* \sim 0.1$ were almost equal (and differing only by ~ 0.002).

We are thankful to Michael Eisenbach for helpful discussions and to Howard C. Berg for his comments on the manuscript.

This work was supported by a grant from the Tel Aviv University Research Authority and by fellowships from the Wolfson and Alon Foundations to N.B.-T.

REFERENCES

Alon, U., L. Camarena, M. G. Surette, Y. Aguera, B. Arcas, Y. Liu, S. Leibler, and J. B. Stock. 1998. Response regulator output in bacterial chemotaxis. *EMBO J.* 17:4238–4248.

Alon, U., M. G. Surette, N. Barkai, and S. Leibler. 1999. Robustness in bacterial chemotaxis. *Nature.* 397:168–171.

Armitage, J. 1993. Methylation-independent behavioral responses in bacteria. *In* Signal Transduction: Prokaryotic and Simple Eukaryotic Systems. J. Kuriyan and B. L. Taylor, editors. Academic Press, Inc., . 43–62.

Asakura, S., and H. Honda. 1984. Two-state model for bacterial chemoreceptor proteins. The role of multiple methylation. *J. Mol. Biol.* 176: 349–367.

Barkai, N., and S. Leibler. 1997. Robustness in simple biochemical networks. *Nature.* 387:913–917.

Barkai, N., and S. Leibler. 1998. Bacterial chemotaxis. United we sense. . . . *Nature.* 393:18–21.

Berg, H. C., and D. A. Brown. 1972. Chemotaxis in *Escherichia coli* analysed by three-dimensional tracking. *Nature.* 239:500–504.

Blat, Y., B. Gillespie, A. Bren, F. W. Dahlquist, and M. Eisenbach. 1998. Regulation of phosphatase activity in bacterail chemotaxis. *J. Mol. Biol.* 284:1191–1199.

Block, S. M., J. E. Segall, and H. C. Berg. 1983. Adaptation kinetics in bacterial chemotaxis. *J. Bacteriol.* 154:312–323.

Bray, D. 1995. Protein molecules as computational elements in living cells. *Nature.* 376:307–312.

Bray, D., and R. B. Bourret. 1995. Computer analysis of the binding reactions leading to a transmembrane receptor-linked multiprotein complex involved in bacterial chemotaxis. *Mol. Biol. Cell.* 6:1367–1380.

Bray, D., R. B. Bourret, and M. I. Simon. 1993. Computer simulation of the phosphorylation cascade controlling bacterial chemotaxis. *Mol. Biol. Cell.* 4:469–482.

Bray, D., M. D. Levin, and C. J. Morton-Firth. 1998. Receptor clustering as a cellular mechanism to control sensitivity. *Nature.* 393:85–88.

Bren, A., and M. Eisenbach. 2000. How signals are heard during bacterial chemotaxis: protein–protein interactions in sensory signal propagation. *J. Bacteriol.* 182:6865–6873.

Cluzel, P., M. Surette, and S. Leibler. 2000. An ultrasensitive bacterial motor revealed by monitoring signaling proteins in single cells. *Science.* 287:1652–1655.

Edwards, J. S., R. U. Ibarra, and B. O. Palsson. 2001. In silico predictions of *Escherichia coli* metabolic capabilities are consistent with experimental data. *Nature Biotechn.* 19:125–130.

Eisenbach, M. 1996. Control of bacterial chemotaxis. *Mol. Microbiol.* 20:903–910.

Ellgaard, L., M. Molinari, and A. Helenius. 1999. Setting the standards: quality control in the secretory pathway. *Science.* 286:1882–1888.

Falke, J. J., and G. L. Hazelbauer. 2001. Transmembrane signaling in bacterial chemoreceptors. *Trends Biochem. Sci.* 26:257–265.

Fullekrug, J., and T. Nilsson. 1999. Protein sorting in the Golgi complex. *Biochim. Biophys. Acta.* 1404:77–84.

Gegner, J. A., D. R. Graham, A. F. Roth, and F. W. Dahlquist. 1992. Assembly of an MCP receptor, CheW, and kinase CheA complex in the bacterial chemotaxis signal transduction pathway. *Cell.* 70:975–982.

Hauri, D. C., and J. Ross. 1995. A model of excitation and adaptation in bacterial chemotaxis. *Biophys. J.* 68:708–722.

Huang, C., and R. C. Stewart. 1993. CheZ mutants with enhanced ability to dephosphorylate CheY, the response regulator in bacterial chemotaxis. *Biochim. Biophys. Acta.*1202:297–304.

Ibba, M., and D. Soll. 1999. Quality control mechanisms during translation. *Science* 286:1893–1897.

Lamb, T. D. 1996. Gain and kinetics of activation in the G-protein cascade of phototransduction. *Proc. Natl. Acad. Sci. U.S.A.* 93:566–570.

Lauffenburger, D. A. 2000. Cell signaling pathways as control modules: complexity for simplicity? *Proc. Natl. Acad. Sci. U.S.A.* 97:5031–5033.

Li, G., and R. M. Weis. 2000. Covalent modification regulates ligand binding to receptor complexes in the chemosensory system of *Escherichia coli*. *Cell.* 100:357–365.

Liu, Y., M. Levit, R. Lurz, M. G. Surette, and J. B. Stock. 1997. Receptor-mediated protein kinase activation and the mechanism of transmembrane signaling in bacterial chemotaxis. *EMBO J.* 16:7231–7240.

Lybarger, S. R., and J. R. Maddock. 1999. Clustering of the chemoreceptor complex in *Escherichia coli* is independent of the methyltransferase CheR and the methylesterase CheB. *J. Bacteriol.* 181:5527–5529.

Macnab, R. M. 2001. Protein crystal mimics reality. *Nature.* 410:321–322.

McNamara, B. P., and A. J. Wolfe. 1996. Coexpression of the long and short form of CheA, the chemotaxis histidine kinase, by members of the family Enterobacteria. *J. Bacteriol.* 179:1813–1818.

Morton-Firth, C. J., T. S. Shimizu, and D. Bray. 1999. A free-energy-based stochastic simulation of the Tar receptor complex. *J. Mol. Biol.* 286: 1059–1074.

Robinson, V. L., D. R. Buckler, and A. M. Stock. 2000. A tale of two components: a novel kinase and a regulatory switch. *Nature Struct. Biol.* 7:626–633.

Samatey, F. A., K. Imada, S. Nagashima, F. Vonderviszt, T. Kumasaka, M. Yamamoto, and K. Namba. 2001. Structure of the bacterial flagellar protofilament and implications for a switch for supercoiling. *Nature.* 410:331–337.

Sanatinia, H., E. C. Kofoid, T. B. Morrison, and J. S. Parkinson. 1995. The smaller of two overlapping CheA gene products is not essential for chemotaxis in *Escherichia coli. J. Bacteriol.* 177:2713–2720.

Sanna, M. G., and M. I. Simon. 1996. In vivo and in vitro characterization of *Escherichia coli* protein CheZ gain- and loss-of-function mutants. *J. Bacteriol.* 178:6275–6280.

Segall, J. E., S. M. Block, and H. C. Berg. 1986. Temporal comparisons in bacterial chemotaxis. *Proc. Natl. Acad. Sci. U.S.A.* 83:8987–8991.

Segall, J. E., M. D. Manson, and H. C. Berg. 1982. Signal processing times in bacterial chemotaxis. *Nature.* 296:855–857.

Segel, L. A., A. Goldbeter, P. N. Devreotes, and B. E. Knox. 1986. A mechanism for exact sensory adaptation based on receptor modification. *J. Theor. Biol.* 120:151–179.

Sourjik, V., and H. C. Berg. 2000. Localization of components of the chemotaxis machinery of *Escherichia coli* using fluorescent protein fusions. *Mol. Microbiol.* 37:740–751.

Spiro, P. A., J. S. Parkinson, and H. G. Othmer. 1997. A model of excitation and adaptation in bacterial chemotaxis. *Proc. Natl. Acad. Sci. U.S.A.* 94:7263–7268.

Stock, J. B., G. Kersulis, and D. E. Koshland, Jr. 1985. Neither methylating nor demethylating enzymes are required for bacterial chemotaxis. *Cell.* 42:683–690.

Stock, J. B., and M. G. Surrete. 1996. Chemotaxis. *In Escherichia coli* and Salmonella: Cellular and Molecular Biology. F. C. Neidhardt, editor. American Society for Microbiology, Washington, DC. 1103–1129.

Turner, L., W. S. Ryu, and H. C. Berg. 2000. Real-time imaging of fluorescent flagellar filaments. *J. Bacteriol.* 182:2793–2801.

Wang, H., and P. Matsumura. 1996. Characterization of the CheAS/CheZ complex: a specific interaction resulting in enhanced dephosphorylating activity on CheY-phosphate. *Mol. Microbiol.* 19:695–703.

Wang, H., and P. Matsumura. 1997. Phosphorylating and dephosphorylating protein complexes in bacterial chemotaxis. *J. Bacteriol.* 179: 287–289.

Yi, T. M., Y. Huang, M. I. Simon, and J. Doyle. 2000. Robust perfect adaptation in bacterial chemotaxis through integral feedback control. *Proc. Natl. Acad. Sci. U.S.A.* 97:4649–4653.